Available online at www.sciencedirect.com
ScienceDirect
Sensors and Actuators B 122 (2007) 659–671
SENSORS AND ACTUATORS B CHEMICAL
www.elsevier.com/locate/snb

Review

# Chemical sensors based on nanostructured materials

Xing-Jiu Huang, Yang-Kyu Choi *

*Nano-Bio-Electronic Lab, Department of Electrical Engineering and Computer Science, Korea Advanced Institute of Science and Technology, 373-1 Guseong-dong, Yuseong-gu, Daejeon, South Korea*

Received 31 March 2006; received in revised form 13 June 2006; accepted 13 June 2006
Available online 24 July 2006

**Abstract**

This article provides a comprehensive review of current research activities that concentrate on chemical sensors based on nanotubes, nanorods, nanobelts, and nanowires. We devote the most attention on the experimental principle, design of sensing devices, sensing mechanism, and some important conclusions. We elaborate on development of chemical sensors based on nanostructured materials in the following four sections: (1) nanotube sensors; (2) nanorod sensors; (3) nanobelt sensors; (4) nanowire sensors. We conclude this review with personal perspectives on the directions towards which future research on nanostructured sensors might be directed.


*Keywords:* Chemical sensors; Nanotubes; Nanorods; Nanobelts; Nanowires

## Contents



## 1. Introduction

The most important aspect of investigation of a variety of sensors is 3 'S', i.e. sensitivity, selectivity, and stability. Up to now, great efforts have been made to better resolve these problems, such as research on novel sensing materials research [1–3], data analytical method (FFT and wavelet transform, pattern recognition) [4,5], measurement techniques (static and dynamic) [6–9], control of sensors structures (arrays) [10,11], sensor fabrication techniques [12–17], surface modification [18,19], etc. With the development of nano-science and technology, a large number of literatures on one-dimensional nanostructured materials,

* Corresponding author. Tel.: +82 42 869 3477; fax: +82 505 869 3477.
*E-mail address:* ykchoi@ee.kaist.ac.kr (Y.-K. Choi).

0925-4005/$ – see front matter © 2006 Elsevier B.V. All rights reserved.
doi:10.1016/j.snb.2006.06.022

including tubes, rods, belts, and wires in this area, have been published every year. These materials have their unique structure; it is evident that the structure of nanowires and nanorods is similar to each other which are dominated by a wire-like structure whose diameter varies over a broad range from several tens of nanometers to a micrometer. The typical length of the nanowires ranges from several tens to several hundred micrometers, whereas the length of nanorods is only several micrometers. TEM observation indicates that nanotubes possess the wire-like nanostructures with hollow cores. Considering the contrast over the length of the nanostructure and the results of chemical imaging, the belt-like nanostructure is found to have a rectangular cross-section. Each nanobelt has a uniform width along its entire length, and the typical widths of the nanobelts are in the range of several tens to several hundred nanometers. Due to their interesting structures, it provides many opportunities to study their interesting sensing behavior by making new types of nanosensing structures. In this article, we give a comprehensive review of current research activities that concentrate on chemical sensors based on nanotubes, nanorods, nanobelts, and nanowires. Due to the large amount of literatures, the following narrative highlights researches published in the past 5 years in this busy field. Though sensor applications of carbon nanotubes have been researched by a number of authors, we intend to exclude them from the scope of this article. This review is divided into four sections. In each section, we focus on the experimental principle, design of sensing devices, sensing mechanism, and some important conclusions. The article concludes with a brief comments and outlook concerning the sensor application of one-dimensional nanomaterials.

## 2. Nanotube sensors

In general, nanotube-based sensors include metal oxide tubes such as $Co_3O_4$, $Fe_2O_3$, $SnO_2$, and $TiO_2$ and metal tubes such as Pt nanosensor.

Li et al. [20] presented that $Co_3O_4$ nanotubes exhibited superior gas sensing capabilities towards $H_2$. The sensor was fabricated by casting the mixture of nanotubes and ethanol on ceramic tubes with the connection through gold electrodes that were connected by four platinum wires. They suggested that the change of resistance was mainly caused by the adsorption and desorption of gas molecules on the surface of the sensing structure; the hollow inside the tubes and the porous surface of the $Co_3O_4$ nanotubes could provide more active sites in the three dimensional structure, and enabled the detecting gases to access more surfaces. They also found that $\alpha$-$Fe_2O_3$ exhibited high sensitivity to $H_2$ and $C_2H_5OH$ at room temperature [21].

Recently, Liu and Liu [22] reported a single square shaped $SnO_2$ nanotube gas sensor to ethanol which was bridged to two interdigitated Pt electrodes. They suggested that the advantages included the dramatically accelerated transport of gas/liquid in and out of the box beams, significantly increased active surface areas and increased flexibility in surface modification for chemically or biologically selective catalysis, drastically enhanced transport of ionic and electronic defects in the solid state (perpendicular to the wall thickness) due to shorter diffusion lengths, radically increased population of defects at surfaces/interfaces for fast electrode kinetics, and quantum interactions at the nanoscale. Huang et al. [23] studied responses of a $SnO_2$ nanotube sheet sensor to 100 ppm $H_2$, 100 ppm CO, and 20 ppm ethylene oxide. The sheet (0.2 mm in thick) was of about 2 mm × 4 mm in size and was fixed with gold paste onto an alumina substrate attached with gold electrodes having a gap of 1 mm.

Also of interest is the research of Grimes and co-workers [24–27] who described a room temperature hydrogen sensor comprised of a $TiO_2$ nanotube array capable to recover substantially from sensor poisoning through ultraviolet (UV) photocatalytic oxidation of the contaminating agent. A 10 nm coating of Pd was evaporated onto the surface of the titania nanotube array film to enhance the hydrogen sensitivity of the sensor, which showed over a 170,000% change in electrical resistance upon exposure to 1000 ppm hydrogen at 24 °C. They suggested that adsorbed oxygen played a major role in manipulating the conductivity. On UV illumination, the chemisorbed oxygen must be desorbed, increasing the conductivity. Hence, the conductivity increase upon UV exposure has one part from the photogenerated current and another part from the electrons donated by the desorbed oxygen. On removing the UV illumination, oxygen will be re-adsorbed and hence the electrons will be extracted from the sensor. However, the process of oxygen re-adsorption is slow, on the order of several minutes, and hence it takes a relatively long time to regain the original sensor resistance after the UV illumination is removed.

Xia and co-workers [28] systematically investigated the glucose electrochemical-sensing behavior directly using highly ordered platinum-nanotube array electrodes (NTAEs) supported on a gold substrate. The authors suggested that NTAEs were easily regenerated by electrochemical cleaning, and were mechanically and chemically stable. Meanwhile, NTAEs retain high sensitivity in the presence of chloride ions, which is essential for use as enzyme-free electrochemical sensors. Such a glucose sensor allows the determination of glucose in a linear range of 2–14 mM, with a sensitivity of 0.1 $\mu A\,cm^{-2}\,mM^{-1}$ and a detection limit of 1.0 $\mu$M glucose, with negligible interference from physiological levels of 0.1 mM *p*-acetamedophenol, 0.1 mM ascorbic acid, and 0.02 mM uric acid.

## 3. Nanorod sensors

Generally a large number of repetitive steps of nanorod-based sensors are involved in metal oxide nanorods such as ZnO, $MoO_3$, and tungsten oxide nanosensors, polymer nanorods such as poly(3,4-ethylene-dioxythiophene) nanosensor, and metal nanorods such as Au nanosensor. Among these researches, most attention has been focused on ZnO nanorods sensors.

Wang and co-workers [29,30] fabricated thick film sensors based on ZnO nanorods. The paste prepared from a mixture of ZnO nanorods with a polyvinyl alcohol solution was coated onto an $Al_2O_3$ tube on which two gold leads had been installed at each end. A heater of Ni–Cr wire was inserted into the $Al_2O_3$ tube to supply the operating temperature which was controlled in the range of 100–500 °C. The nanorod sensors could detect 1 ppm

$C_2H_5OH$ (350 °C) and 0.05 ppm $H_2S$ (25 °C). They suggested that the gas response was mainly dependent upon two factors. The first is the amount of active sites for oxygen and the reducing gases on the surface of the sensor materials. The more active sites the surface of nanosensor contain, the higher sensitivity the sensor exhibits. The second is the reactivity of the reducing gases. The bond energy of H–SH is 381 kJ/mol [31], so that it is easy to open the bond H–SH at lower temperature. On the other hand, the bond energies $H–CH_2$, $H–OC_2H_5$ and H–CH in $C_2H_5OH$ are 473, 436 and 452 kJ/mol [31], respectively, so that it is difficult to open the bonds in $C_2H_5OH$ at lower temperature. Kang et al. [32] reported that multiple ZnO nanorods are sensitive to $H_2$ at 112 °C or $O_3$ at room temperature. They also found that ZnO nanorods showed dramatic changes in conductance upon exposure to polar liquids [33]. The results indicate the possibility of functionalizing the surface for application as biosensors, especially given the excellent biocompatibility of the ZnO surfaces, which should minimize degradation of adsorbed cells. Wang and co-workers presented the sensitivity to 10 ppm $H_2$ and 1000 ppm $C_2H_5OH$ of Pd/multiple [34] and multipod shaped [35] ZnO nanorods sensors. The dominant mechanism for this sensing process is more likely to be the chemisorption of hydrogen on the Pd surface. Multipod ZnO nanorods which have more than four even tens of needle-like nanorods [36] at a common junction resulted in a very large surface area, and therefore their sensing properties related to the surface reactions could be greatly enhanced. Xu et al. [37,38] found the treatment process of ZnO nanorods had obvious effect on its gas sensing properties to HCHO, LPG, and $H_2S$.

Zhang et al. [39] reported ZnO nanorods for a reagentless uric acid biosensor. The uricase/ZnO biosensor was constructed by casting uricase on the ZnO membrane. The electrocatalytic response showed a linear dependence on the uric acid concentration ranging from $5.0 \times 10^{-6}$ to $1.0 \times 10^{-3}$ M with a detection limit of 2 μM. In their work, ZnO nanorods played the role of an efficient electron-conducting tunnel and had a very high specific surface area. Consequently, the uricase attached to the ZnO nanorods surface had more spatial freedom in its orientation, which facilitated the direct electron transfer between the active sites of the immobilized uricase and the electrode surface.

Comini et al. [40] presented the high sensitivity of a $MoO_3$ nanorods film sensor to 30 ppm carbon monoxide and 100 ppm ethanol. Kim et al. [41] studied a gas sensor based on a nonstoichiometric tungsten oxide nanorod film. The sensor was fabricated on Si wafers as the substrates by using microelectromechanical system (MEMS) and silicon technology. The authors measured the sensor responses to 2% $N_2$ (or air), 1000 ppm ethanol, 10 ppm $NH_3$, and 3 ppm $NO_2$ in both dry air and nitrogen atmosphere at room temperature. Their response magnitudes ascend in the order of air, $C_2H_5OH$, $NH_3$, and $NO_2$ exposures.

Sudeep et al. [42] reported a novel strategy for the selective detection of micromolar concentrations of cysteine (3 μM) and glutathione (12 μM) by exploiting the interplasmon coupling in Au nanorods. Firstly, the thiol group of cysteine/glutathione molecules is selectively functionalized onto the edges of Au nanorods, leaving the zwitterionic groups for further interaction. Secondly, the appended zwitteronic groups at the ends of Au nanorods assist the coupling through a two-point electrostatic interaction in a cooperative fashion. Sönnichsen and Alivisatos [43] reported an ideal probe for orientation sensing in material science and molecular biology by monitoring the polarized light scattering from individual gold nanorods in a darkfield microscope.

Jang et al. [44] presented a poly(3,4-ethylene-dioxythiophene) (PEDOT) nanorods nanosensor and used it for the detection of HCl and $NH_3$ vapor. The PEDOT nanorode sensors gave a measurable response to $NH_3$ and HCl vapor concentration as low as 10 and 5 ppm, respectively. The recovery time of PEDOT nanorod sensors for $NH_3$ and HCl was about 70 and 80 s, respectively.

## 4. Nanobelt sensors

As for nanobelt-based sensors, the main attentions have been focused on metal oxides such as ZnO, $SnO_2$ and $V_2O_5$ nanosensors, especially on ZnO nanobelts sensors. The ability of $SnO_2$ field-effect transistors to act as oxygen sensors is demonstrated by Wang and co-workers [45]. They have also assembled tin dioxide nanobelts with low-power microheaters for detecting dimethyl methylphosphonate, a nerve agent stimulant [46]. A focused ion beam method was used to deposit a thin Pt coating on the contact location between the nanobelt and each Pt electrode so as to improve the electrical contact. Again, they reported gas sensors to detect environmental polluting species based on single $SnO_2$ nanobelts, like CO and $NO_2$ sensors, ethanol sensors for breath analyzers, and food sensors [47]. The detection limit reaches the level of a few ppb.

Yang and co-workers [48] reported photochemical $NO_2$ sensors based on individual single-crystalline $SnO_2$ nanoribbons that worked at room temperature. The resolution limit of the sensor was 5–10 ppm. They further [49] found that $SnO_2$ nanoribbons with exposed $(1\,0\,\bar{1})$ and $(0\,1\,0)$ surfaces were highly effective $NO_2$ sensors at room temperature. The sensing mechanism was examined through the first principles of density functional theory (DFT) calculations. Kolmakov et al. [50] investigated the sensing ability of individual $SnO_2$ nanobelts before and after functionalization with Pd catalyst particles. The Pd-functionalized nanostructures exhibited a dramatic improvement in sensitivity toward oxygen and hydrogen due to the enhanced catalytic dissociation of the molecular adsorbate on the Pd nanoparticle surfaces and the subsequent diffusion of the resultant atomic species to the oxide surface. Faglia et al. [51] presented that the visible photoluminescence (PL) of $SnO_2$ nanobelts could be quenched by nitrogen dioxide at a ppm level in a fast (time scale order of seconds) and reversible way. $NO_2^-$ involved surface states responsible for PL quenching are probably the ones with lower binding energies and negligible net charge transfer that could easily and quickly be adsorbed and desorbed from the oxide surface, such as the species $[NO_2]_{2,Sn,O}$ identified by Maiti et al. [49]. Gao and Wang [52] found that the $SnO_2$ nanobelt/CdS nanoparticle core/shell heterostructured sensor had high sensitivity to 100 ppm ethanol vapors in air at 400 °C. The authors suggested that the CdS nanoparticles would have served as additional electron sources that greatly improved

the electron conduction in the $SnO_2$ nanobelts. Kong and Li [53] presented a highly sensitive and selective CuO–$SnO_2$ sensor to $H_2S$ based on $SnO_2$ nanoribbons. Comini et al. [54] proposed a $SnO_2$ nanobelts film for gas sensing and proved its capability to reveal of gases like 30 ppm CO (350 °C), 200 ppb $NO_2$ (300 °C), and 10 ppm ethanol (350 °C).

A novel highly selective and stable ethanol sensor based on single-crystalline divanadium pentoxide nanobelts was reported by Li and co-workers [55]. The $V_2O_5$ nanobelts showed greater sensitivity to ethanol of either low (<10 ppm) or high (1000 ppm) concentrations. The response and recovery times were 30–50 s.

## 5. Nanowire sensors

### 5.1. Metal nanowire sensors

Penner and co-workers [56] reported hydrogen sensors and switches based on electrodeposited palladium mesowire arrays (PMAs). These sensors consisted of up to 100 Pd mesoscopic wires (henceforth, "mesowires") arrayed in parallel (Fig. 1, left, A and B), which contacted with silver epoxy. A rise-time (baseline to 90% signal saturation) of less than 80 ms was observed for the response of the mesowire-based sensors to 5% $H_2$. They suggested that the hydrogen sensing mechanism of the wire-based sensor was based on the resistivity changes caused not by the surface adsorption but by the structure changes of the wire itself, as shown in Fig. 1 (right). After the first exposure to $H_2$, exposure to air opened the nanoscopic gaps in some or all mesowires in the sensor. These gaps opened when the hydrogen-swollen Pd grains in each mesowire returned to their equilibrium dimensions in the absence of hydrogen. Subsequently, it was the closing of these gaps or "break junctions" in the presence of $H_2$ that accounted for the decreased resistance of the sensor. Many or all of the mesowires in the array exhibited this kind of switching behavior. Penner and co-workers [57,58] also demonstrated that the ensembles of silver mesowires with diameters ranging from 150 to 950 nm and lengths of 100 μm or more showed a resistance increase, fast (<5 s), and reversible, upon exposure to ammonia ($NH_3$).

Pd nanowire-based hydrogen sensors and polypyrrole nanowire-based pH sensors were demonstrated by Yun et al. [59]. Using a single electrodeposited Pd wire with a 1 μm diameter and a 7 μm length, they demonstrated the sensing of hydrogen gas of different concentrations (1–3% in $N_2$ gas). Similarly, Atashbar and Singamaneni [60] investigated a room temperature hydrogen gas sensor based on palladium nanowires.

Yang et al. [61] demonstrated the capability of silver nanowire substrates for the detection of 2,4-dinitrotoluene (2,4-DNT), the most common nitroaromatic compound for detecting buried landmines, and other explosives by utilizing vibrational signatures. The sensitivity of about 0.7 pg was achieved.

Tao and co-workers [62] studied the sensing behaviors of Cu nanowire arrays in solutions of three molecules; 2,2′-bipyridine (22BPY), adenine, and mercaptopropionic acid (MPA). They demonstrated that the mechanism depended on the molecule–nanowire interactions and the conductance changes should be specific for different adsorptions. The specificity can be improved if the nanowires are pre-adsorbed with functionalized molecules because a specific interaction of a sample molecule with the functionalized molecules provides identity information about the sample molecule.

### 5.2. Silicon nanowire nanosensors

Lieber's group has done a series of excellent works for silicon nanowire-based sensors. They presented highly sensitive and real-time sensors based on electrically boron-doped silicon nanowires (SiNWs) for detecting a biological and chemical

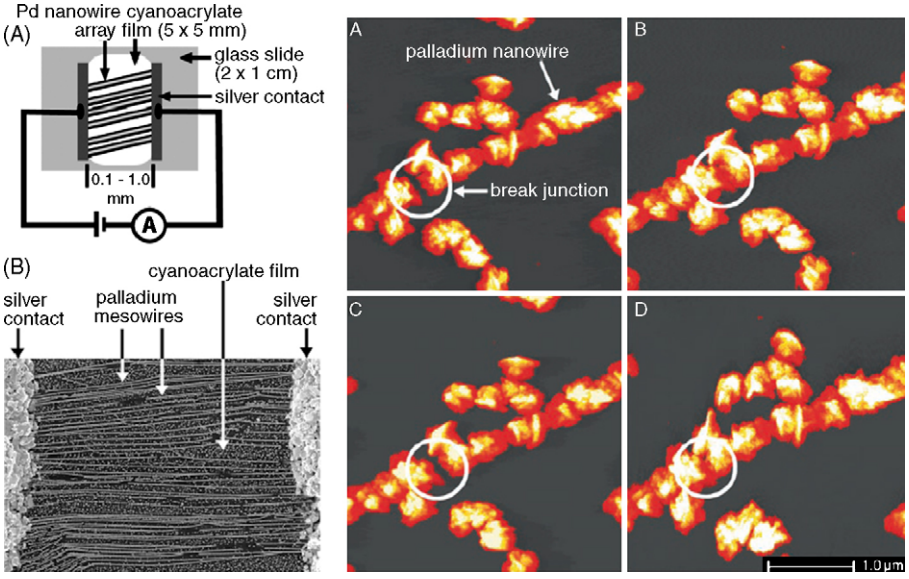


Fig. 1. (Left) (A) Schematic diagram of a PMA-based hydrogen sensor or switch. (B) SEM image of the active area of a PMA-based hydrogen sensor. (Right) Atomic force microscope images of a Pd mesowire on a graphite surface. Images (A) and (C) were acquired in air, and images (B) and (D) were acquired in a stream of hydrogen gas. A hydrogen-actuated break junction is highlighted.

species, amine, and the oxide-functionalized SiNWs exhibited pH-dependent conductance that was linear over a wide dynamic range [63].

They evaluated the response the of 3-aminopropyltriethoxysilane-modified SiNW to changes in solution pH by fabricating a cell consisting of a microfluidic channel formed between a poly(dimethylsiloxane) mold and the SiNW/substrate [64]. Continuous flow or static experiments demonstrated that the SiNW conductance increases stepwise with discrete changes in pH from 2 to 9 and that the conductance was constant for a given pH; the changes in conductance were also reversible for increasing and/or decreasing the pH. These results could be understood by considering the change in surface charge during protonation and deprotonation after the surface functionality of the modified SiNWs. To explore biomolecular sensors, they functionalized SiNWs with biotin and studied the well-characterized ligand–receptor binding of biotin–streptavidin. Measurements showed that the conductance of the biotin-modified SiNWs increased rapidly to a constant value upon addition of a 250 nM streptavidin solution and that this conductance value was maintained after the addition of a pure buffer solution. They confirmed that the observed conductance changes were due to the specific binding of streptavidin to the biotin ligand.

Hahm and Lieber [65] also demonstrated that p-type SiNWs functionalized with peptide nucleic acid (PNA) receptors functioned as ultrasensitive and selective real-time DNA sensors at concentrations down to tens of femtomolar range. Direct, real-time electrical detection of single virus particles with high selectivity by using nanowire field-effect transistors was also reported by Lieber and co-workers [66]. Measurements made with nanowire arrays modified with antibodies for influenza A showed discrete conductance changes characteristic of binding and unbinding in the presence of influenza A but not paramyxovirus or adenovirus. The authors suggested that the conductance of that device should change from the baseline value when a virus particle was bound to the antibody receptor on a nanowire device, and the conductance should return to the baseline value when the virus was unbound. Fig. 2 shows the parallel collection of conductance, fluorescence, and right-field data from a single nanowire device with fluorescently labeled viruses.

They continued to study a highly sensitive detection scheme for identifying small molecule inhibitors that did not require labeling of the protein, ATP, or small molecule and could be carried out in real-time by using SiNWs field-effect transistor (FET) devices [67]. They linked the Abl tyrosine kinase to the surface of SiNWs FET within microfluidic channels to create active electrical devices and investigated the binding of ATP and competitive inhibition of ATP binding with organic molecules, as shown schematically in Fig. 3 (left bottom). Plots of the normalized conductance versus time recorded from the Abl-modified SiNW devices (Fig. 3, right) exhibit reversible decreases in conductance due to competitive inhibition of ATP binding by small molecules.

Many interesting works on silicon nanowire-based nanosensors have also been reported by other group. Lee and co-workers [68] studied the chemical sensitivity of SiNWs bundles upon exposure to ammonia gas and water vapor. The sensors were made by pressing bundles of HF- and non-etched Si nanowires of

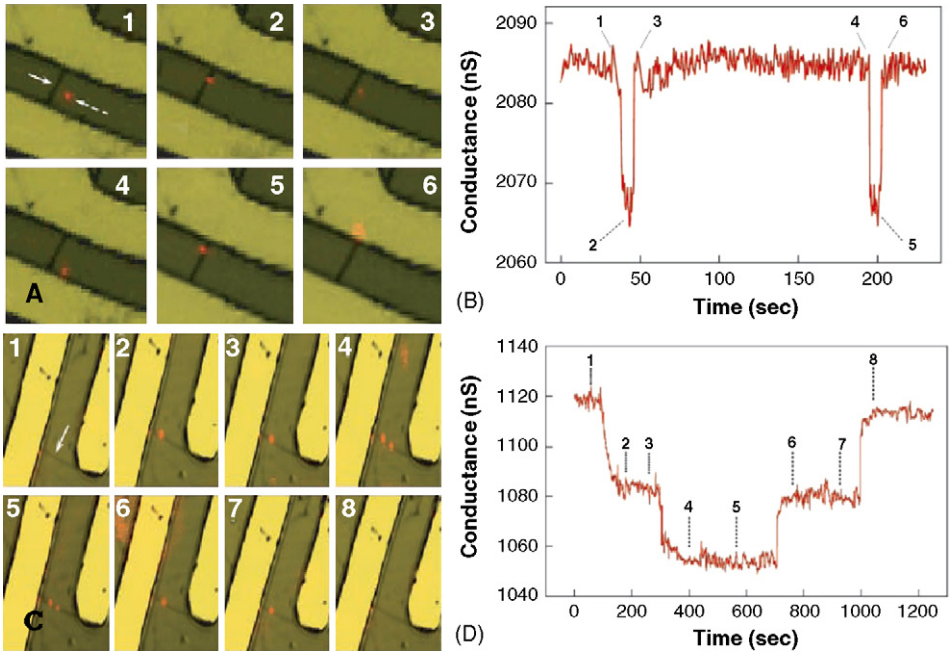


Fig. 2. Selective detection of single viruses. (A) Optical and (B) conductance data recorded simultaneously versus time for a single silicon nanowire device after introduction of influenza A solution. Combined bright-field and fluorescence images correspond to time points 1–6 indicated in the conductance data; virus appears as a red dot in the images. The solid white arrow in image 1 (A) highlights the position of the nanowire device, and the dashed arrow indicates the position of a single virus. Images are 8 μm × 8 μm. All measurements were performed with solutions containing 100 viral particles per microliter. (C) Optical and (D) simultaneous conductance vs. time data recorded from a single nanowire device with a high density of anti-influenza type A antibody. Influenza A solution was added before point 1, and the solution was switched to pure buffer between points 4 and 5 on the plot. The bright-field and fluorescence images corresponding to time points 1–8 are indicated in the conductance data; the viruses appear as red dots in the images. Each image is 6.5 μm × 6.5 μm.

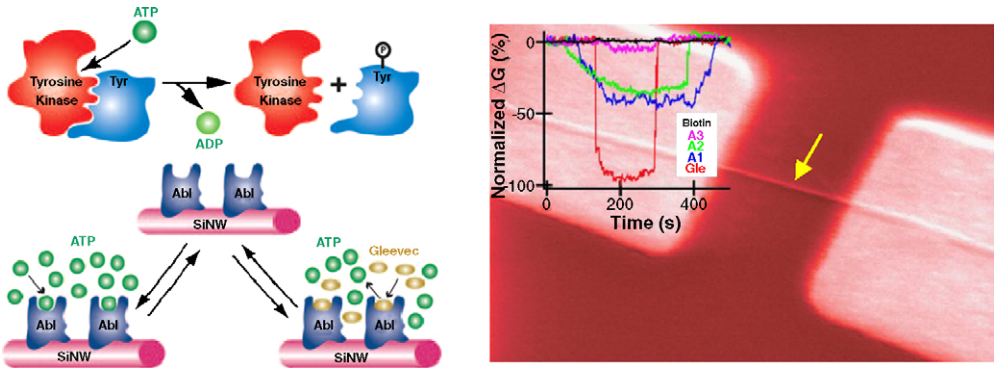


Fig. 3. Detection of small molecule–protein interactions for tyrosine kinases. (Left, top) Scheme illustrating basic activity of a tyrosine kinase: ATP binds to the tyrosine kinase active site, and then the γ-phosphate group is transferred to the tyrosine (Tyr) residue of the substrate protein. (Bottom) Detection of ATP binding and small molecule inhibition of binding by using a SiNW sensor device. The tyrosine kinase Abl is covalently linked to the surface of a SiNW, and then the conductance of the nanowire device is monitored to detect ATP binding and the competitive inhibition of ATP binding by Gleevec. (Right) Scanning electron micrograph of a typical SiNW FET device. The nanowire is highlighted by a yellow arrow and is contacted on either end of Ti–Au metal electrodes. (Inset) Normalized conductance vs. time data recorded from Abl-modified SiNW devices by using solutions containing 100 nM ATP and 50 nM small molecules for Gleevec (red), A1 (blue), A2 (green), A3 (pink), and biotin (black). (For interpretation of the references to color in this figure legend, the reader is referred to the web version of the article.)

about 0.4 mg onto the surface of insulating glasses. The sensing mechanism could be understood according to two possible ways, i.e. the contact resistance across two nanowires and the surface resistance along the individual nanowire. Bashir and co-workers [69] described silicon nanowire oxygen sensor that was realized using top–down microelectronics processing techniques. Unlike the idea of Lieber's group, Hsu et al. [70] presented a SiNW-based pH sensor in an extended-gate field-effect transistor. They suggested that SiNWs could support a three-dimensional contact mode, resulting in a larger total surface area, and the SiNWs were cylindrical, which caused the non-bridging Si–O bonds of the surface to be of the suspended and standing types.

Li et al. [71,72] reported sequence-specific label-free DNA sensors based on SiNWs with peptide nucleotide acid (PNA) or single-stranded (ss) probe DNA molecules covalently immobilized on the nanowire surfaces. Label-free complementary (target) ss-DNA in sample solutions were recognized when the target DNA was hybridized with the probe DNA attached on the SiNW surfaces, producing a change of the conductance of the SiNWs. For a 12-mer oligonucletide probe, 25 pM of the target DNA in solution was detected easily (signal/noise ratio > 6), whereas 12-mer with one base mismatch did not produce a signal above the background noise. Sheu et al. [73] demonstrated molecular detection based on SiNWs whose surface was pretreated by *N*-(2-aminoethyl)-3-aminopropyl-trimethoxysilane and then selectively deposited with gold nanoparticles. The gold nanoparticles deposited on the oxide surface of the SiNWs and then functionalized with amino groups served as linkers to detect molecules. The target molecules, such as $\Delta^5$-3-ketosteroid isomerase (KSI-126C) molecules, bound with gold nanoparticles on the surface of the SiNWs and resulted in a voltage shift.

Tong and co-workers [74] proposed to use single-mode subwavelength-diameter silica nanowires for optical sensing based on evanescent-wave guiding properties of the nanowire waveguides. The phase shift of the guided mode caused by index change was obtained by solving Maxwell's equation, and was used as a criterion for sensitivity estimation. A nanowire sensor employing a wire assembled Mach–Zehnder structure was modeled. This silicon nanowire-based optical sensing may suggest a new approach to miniaturized optical sensors with high sensitivity. However, there are still some problems to be considered in the future such as instability of the nanowire-assembled couplers and oversensitivity of the whole system. The schematic diagram of the functionalized nanowire waveguides as sensing elements for detecting specimens in aqueous solutions is shown in Fig. 4.

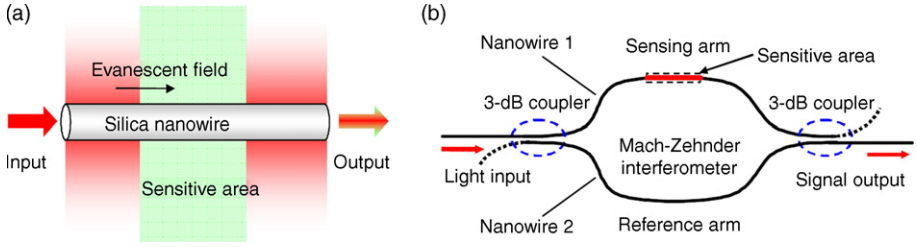


Fig. 4. (a) A silica nanowire sensing element exposed to or immersed in the solution to be detected (highlighted in light green), and the wire guides light as a single-mode waveguide. (b) A proposed sensor with a Mach–Zehnder interferometer. A Mach–Zehnder interferometer can be assembled with two uniform silica nanowires; nanowire 1 is used as a sensing arm with a certain length of sensitive area exposed to the measurand, and nanowire 2 is used as a reference arm that is kept under constant condition and is isolated from the measurand. (For interpretation of the references to color in this figure legend, the reader is referred to the web version of the article.)

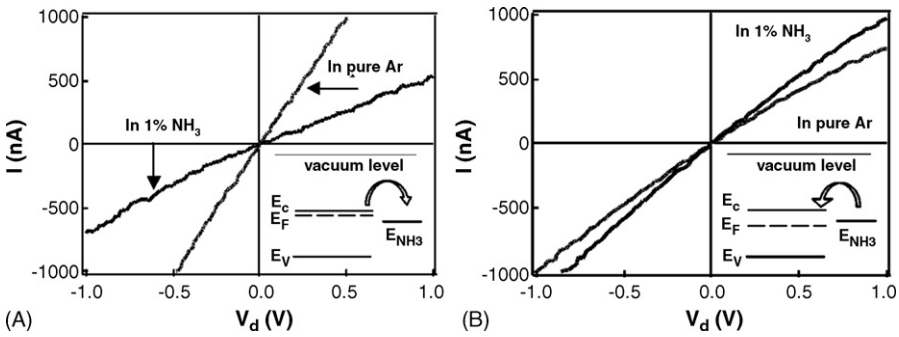


Fig. 5. (A) $I-V_d$ curves of sample 1 before and after exposure to 1% $NH_3$. (Inset) Energy band diagrams of heavily doped $In_2O_3$ and $NH_3$ molecules. (B) $I-V_d$ curves of sample 2 before and after exposure to 1% $NH_3$. (Inset) Energy band diagrams of lightly doped $In_2O_3$ and $NH_3$ molecules.

### 5.3. Metal oxide nanowire sensors

#### 5.3.1. $In_2O_3$ nanowire sensors

Zhang and co-workers have done a series of wonderful works for $In_2O_3$ nanowire-based sensors. They demonstrated a single $In_2O_3$ nanowire to work as chemical sensors for $NO_2$ and $NH_3$ at room temperature [75]. The devices showed responses (defined as the resistance after exposure divided by the resistance before exposure) as high as $10^6$ for diluted $NO_2$ and $10^5$ for diluted $NH_3$. The response times (defined as the time duration for resistance change by one order of magnitude) were determined to be 5 s for 100 ppm $NO_2$ and 10 s for 1% $NH_3$, and the lowest detectable concentrations were 0.5 ppm for $NO_2$ and 0.02% for $NH_3$. Continuously, they observed changes of conductance in opposite directions with different nanowire sensors [76,77]. They explained this case using a doping-dependent sensing mechanism; they suggested that the $NH_3$-sensing behavior of $In_2O_3$ nanowires was related to their oxygen vacancy doping concentrations. Figs. 5A and B shows the $I-V_d$ curves before and after exposure to 1% $NH_3$ and the corresponding energy band diagrams for samples 1 and 2, respectively, where $E_c$, $E_v$ and $E_F$ correspond to the conduction band, the valence band and the Fermi level of the $In_2O_3$ nanowires. Once $NH_3$ molecules adsorb onto the $In_2O_3$ nanowire surface, electron transfer proceeds from the material with a higher chemical potential to the material with a lower chemical potential until the system reaches equilibrium. The hypothesis is that for sample 1, the heavily doped device, the nanowire Fermi level $E_F$ is fairly close to the conduction band and located above $E_{NH3}$ (shown in the inset in Fig. 5A). Therefore, electrons should migrate from the nanowire to the adsorbed $NH_3$ species and result in a reduction in the nanowire carrier concentration. This effectively leads to the observed suppressed conductance for sample 1. In contrast, a relatively low doping concentration has been found for sample 2, suggesting that $E_F$ is well below the conduction band, presumably even below $E_{NH3}$ (the inset in Fig. 5B). As a result, electrons transfer from the adsorbed $NH_3$ molecules into the $In_2O_3$ nanowire and hence the enhanced conduction is observed after the exposure. This hypothesis is backed by calculation of the difference between $E_c$ and $E_F$ values for samples 1 and 2, which is estimated to be

$$(E_c - D_F)_{sampl1} - (E_c - E_F)_{sample2} = kT\ln(n_2/n_1) = 81.1\ \text{meV}$$

where $n_1$ and $n_2$ are the electron concentration for samples 1 and 2, respectively. This value is significant even at room temperature and may very well cause the electron transfer in opposite directions for nanowires with different doping concentrations.

Zhou and co-workers [78] also continuously demonstrated detection of $NO_2$ down to ppb levels using transistors based on both single and multiple $In_2O_3$ nanowires operating at room temperature. The multiwire sensor showed an even lower detection limit of 5 ppb, compared to the 20 ppb limit of single nanowire sensors. This room temperature detection limit is the lowest level so far achieved with all metal oxide film or nanowire sensors. The authors tentatively attribute this improved sensitivity to the formation of nanowire/nanowire junctions between the metal electrodes, a feature available in the multiple nanowire devices (Fig. 6) but missing in the single nanowire devices. Such junctions, when exposed to $NO_2$, should form a depleted layer around the intersection and thus block the electron flow

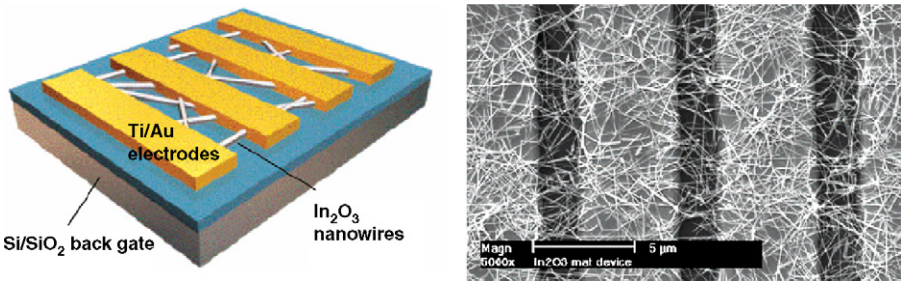


Fig. 6. (Left) Schematic representation of a multiwire device. (Right) Corresponding SEM image of the as-fabricated multiwire devices, where bulk quantities ($10^2$ to $10^3$) of $In_2O_3$ nanowires are contacted by three electrodes.

in a way more prominent than the surface depletion of the single nanowires with metal contacts. When detecting $NO_2$ among other common gases such as $O_2$, CO, and $H_2$ using the multiple nanowire devices, selective response to $NO_2$ was also observed. The authors suggested an "ensemble-averaging effect" as one of possible reasons for the observed high selectivity of the multi-wire sensors. On the basis of their previous study, they suggested that, accordingly, a large ensemble of $In_2O_3$ nanowires, with an appropriate doping level distribution, could have two opposite sensing responses canceling out each other and resulting in the immunity to $NH_3$. This unique property of $In_2O_3$ nanowires offers a new way to achieve selectivity, as compared to the conventional technique of using permeable polymer coatings [79].

Inspired by the aforementioned results, they have explored using $In_2O_3$ nanowires to investigate the chemical gating effect of small organic molecules with amine or nitro groups [80]. The amino groups in both butylamine and 3-(aminoprol) triethoxysilane were found to donate electrons to the n-type $In_2O_3$ nanowires and resulted in enhanced carrier concentrations and also conductance, whereas the nitro groups in butyl nitrite withdrew electrons from the nanowires, and led to reduced carrier concentrations and conduction. To better study the chemical gating effect of low-density lipoproteins (LDL) using $In_2O_3$ nanowires, Zhou et al. studied carbon nanotube transistors as a comparison [81]. The adsorption of LDL on these two different surfaces was investigated, which revealed a tenfold more LDL particle adsorption on carbon nanotubes than on $In_2O_3$ nanowires because of hydrophobic/hydrophilic interactions. The conductance of the field-effect transistors based on the nanowires and nanotubes showed complementary response after the adsorption of LDL: while the $In_2O_3$ nanowire transistors exhibited higher conductance accompanied by a negative shift of the threshold voltage, the carbon nanotube transistors showed lower conductance after the exposure (shown in Fig. 7). This is attributed to the complementary doping type of $In_2O_3$ nanowires (n-type) and carbon nanotubes (p-type).

Zhou and co-workers [82] also achieved the $In_2O_3$ nanowire surface functionalization via a simple and mild self-assembling process, utilizing 4-(1,4-dihydroxybenzene) butyl phosphonic acid (HQ-PA). HQ-PA is an electrochemically active molecule containing a hydroquinone group that undergoes reversible oxidation/reduction at low potentials. Oxidized HQ-PA (Q-PA) reacts with a range of functional groups, which can be easily incorporated into biomolecules and other materials, such as thiols, azides, cyclopentadienes, and primary amines.

Zhou and co-workers investigated not only the chemical- and bio-sensors based on $In_2O_3$ nanowires but also the ultraviolet photodetection properties [83]. They found that $In_2O_3$ nanowire devices exhibited significantly enhanced conduction under UV exposure and high sensitivities were achieved. They believed that two major mechanisms were active in the photoconductive $In_2O_3$ nanowires. First of all, because of the affinity between the electrons and the oxidizing $O_2$ molecules, $O_2$ can adsorb on the nanowire surface and combine with the nearby free electrons to form an $O_2^-$ layer once the nanowire is exposed to air. This reduces the carrier concentration in the n-type $In_2O_3$ nanowire and thus suppresses its conductivity. Upon exposure to UV light, the $O_2^-$ ions will recombine with the photogenerated holes and discharge $O_2$ molecules: $h^+ + O_2^- \rightarrow O_2$. This process helps erase the effect of the surrounding $O_2$ and brings the nanowire to the original electron-rich state. Secondly, further illumination will generate more electron–hole pairs in the conduction and valence bands, and these photogenerated carriers can significantly increase the conductance of the nanowire.

Also, Chu et al. [84] investigated the gas sensing properties of $In_2O_3$ nanowires films. The results revealed that the sensors exhibited higher response and good selectivity to $C_2H_5OH$ at 370 °C. The response time was about 10 s and recovery time was shorter than 20 s.

### 5.3.2. $SnO_2$ nanowire sensors

Moskovits and co-workers [85] reported the $O_2$ and CO sensing properties based on an individual $SnO_2$ nanowire. Exposure to oxygen recreated the surface acceptor states, thereby reducing the nanowire's conductance, and restored the temperature dependence of the conductance to the exponential form typical of

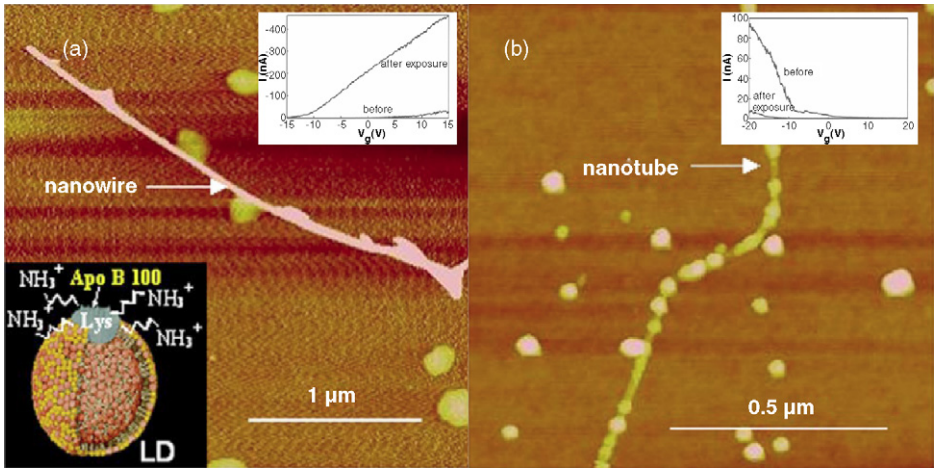


Fig. 7. Typical AFM images of LDL adsorption on an $In_2O_3$ nanowire (a) and a carbon nanotube (b). The inset, $I - V_g$ curves of (a) an $In_2O_3$ nanowire device at $V = -0.1$ V and (b) carbon nanotube transistor at $V = 0.1$ V before and after exposure to LDL.

intrinsic semiconductors. Combustible gases like CO react with pre-adsorbed oxygen species to form carbon monoxide reducing the steady-state surface oxygen concentration and donating a few electrons back into the bulk, and resulting in an increased conductivity which depends monotonically on the gas phase partial pressure of CO. The electron exchange between the surface states and the bulk takes place within a surface layer whose thickness is of the order of the Debye length, $\lambda_D$.

In particular, they presented experimental observations [86] that the rates of oxygen adsorption–desorption and that of the catalytic oxidation of CO, taking place on the surface of a $SnO_2$ nanowire, along with the specific reaction channel, were changed by varying the electron density inside the nanowire, with the help of a gate potential. It was found that manipulating the number of electrons inside a nanowire affected the chemical reactivity and selectivity of its surface.

By close analogy with processes taking place in macroscopic metal oxide semiconductor field-effect transistor (MOSFET) gas sensors, Moskovits' group [87] determined the electron-transport properties of individual tin oxide nanowires configured as FETs over a wide temperature range in various atmospheres comprised of mixtures of $N_2/O_2/CO$. Because of their large surface-to-volume ratios, the bulk electronic properties of the nanowires were found to be controlled almost entirely by the chemical processes taking place at their surface, which could in turn be modified by controlling the gate potential. Thus, the rate and extent of oxygen ionosorption and the resulting rate and extent of catalytic CO oxidation reaction on the nanowire's surface could be controlled and even entirely halted by applying a negative enough gate potential.

Xia and co-workers [88] prepared a polycrystalline $SnO_2$ nanowires film for gas sensing. The nanowire film sensor exhibited high sensitivity and reversibility when exposed to ethanol vapor (∼6%, $V_{ethanol}/V_{air}$), 20 ppm CO, and 500 ppm $H_2$. The authors suggested that this could be attributed to the intrinsically small grain size and high surface-to-volume ratios associated with the polycrystalline nanowires. A thin layer of the film close to the surface could be activated during gas detection due to the dense structure of a compact film. The small grains of $SnO_2$ in the nanowires allowed the sensors to be operated in the most sensitive, grain-controlled mode.

Similarly, Baratto et al. [89] tested the gas sensing of $SnO_2$ nanowires. The response of the sensor was highly selective toward humidity and other polluting species, such as CO and $NH_3$. Wan et al. [90] synthesized Sb-doped $SnO_2$ nanowires and exploited the application for gas sensors. It was found that the response range to ethanol was wide (10–1000 ppm) at 300 °C. The response and recovery times to 10 ppm ethanol were only about 1 and 5 s, respectively. Mulla and co-workers [91] reported the unique response towards $NO_2$ and LPG based on Ru-doped $SnO_2$ nanowires. The nanowires exhibited a highly selective sensing behavior towards $NO_2$ at room temperature.

Mathur et al. [92] studied the photosensing properties of $SnO_2$ nanowires and found that the photoconductance of the $SnO_2$ nanowire showed a strong modulation that was dependent on the average radial dimensions.

*5.3.3. ZnO nanowire sensors*

Wang and co-workers [93] studied the sensing characteristics to ethanol of a ZnO nanowire sensor fabricated with the MEMS technology. It was found that the sensor had a high sensitivity to 200 ppm ethanol at 300 °C. Continuously they fabricated individual ZnO nanowire transistors and characterized them in a vacuum chamber under different oxygen pressures [94]. The transistors exhibited high sensitivity to oxygen, which led to a change of the source drain current and a shift of the threshold voltage. Lu and co-workers [95] also investigated the electrical transport properties of ZnO nanowire FETs. Also, Wang and co-workers [96] fabricated a Cd-doped ZnO nanosensor device using MEMS techniques for humidity detection. Similarly, Zhu et al. [97] found that ZnO nanowires film exhibited high humidity sensitivity, good long-term stability and fast response time.

A ZnO nanowire field-effect chemical sensor and their sensing properties for $NO_2$ and $NH_3$ were presented by Fan and Lu [98]. They observed that the gate potential could affect the detection sensitivity, and the adsorbed gas molecules could be electrically desorbed by applying a large negative gate voltage. Zhang and co-workers [99] studied $NH_3$-sensing characteristics of ZnO nanowires in terms of a quartz crystal microbalance (QCM) at room temperature. The ZnO nanowires showed high sensitivity to ammonia in the range of 40–1000 ppm. The response time was as fast as ∼5 s at any concentration (40–1000 ppm). Meanwhile, they found that the response varied with the thickness of the ZnO nanowires layer. Pearton and co-workers [100] found that single ZnO nanowires coated with Pt clusters by sputtering selectively detected 500 ppm hydrogen at room temperature.

Also, Yang and co-workers [101,102] showed the sensing to ultraviolet light of individual ZnO nanowires.

*5.3.4. Other oxide nanowire sensors*

Yu et al. [103] revealed the effective applications of a two-terminal device fabricated with an individual crystalline β-$Ga_2O_3$ nanowire. The device showed good sensing response to ethanol gas at an operating temperature of 100 °C. The measured response time of the sensor was about 2.5 s. The ethanol concentration changed from 0 to 6000 ppm. Chen and Chen [104] studied the response to CO and ethanol of Ti-doped $Ga_2O_3$ nanowire films. Yu et al. [105] demonstrated the electrical responses of well-aligned $V_2O_5$ nanowires to helium gas and environmental pressures. The authors suggested that the conduction mechanism of the vanadium pentoxide nanowires was related to the modulation of the hopping distance [106], i.e. the hopping distance was shortened by the physical adsorption of the helium gas, whereas it was lengthened by the normal air. $V_2O_5$ nanofibre-based sensors were proven capable of detecting organic amines with extremely high sensitivity and selectivity at room temperature by Vossmeyer and co-workers [107]. The limit of detection for 1-butylamine was found to be less than 30 ppb, which was far below the detection limit of the human olfactory system (ranging from around 240–13.4 ppm [108]). The change of conductance may be attributed to intercalation of the amine into the layered structure of the nanofibres and sorption at the nanofibre/electrode interface.

### 5.4. Polymer nanowire sensors

Yun et al. [59] fabricated a single conducting polypyrrole wire with a 200 nm thickness, a 500 nm width and a 3 μm length, and demonstrated its pH sensing. The conductivity of the polypyrrole wire was directly proportional to the pH.

Kaner and co-workers [109,110] developed polyaniline nanofiber thin film sensors and compared them to conventional polyaniline sensors. They explored five different response mechanisms such as acid doping (HCl), base dedoping ($NH_3$), reduction (with $N_2H_4$), swelling (with $CHCl_3$), and polymer chain conformational changes (induced by $CH_3OH$). Their high surface area, porosity and small diameters enhanced diffusion of molecules and dopants into the nanofibers. When the polyaniline was exposed to HCl, a rapid drop in resistance was observed within a short period of time. This doping of polyaniline is achieved by protonation of the imine nitrogens by HCl. The charge created along the backbone by this protonation was counter-balanced by the resulting negatively charged chloride counterions. The change in conductivity was brought about by the formation of polarons (radical cations) that traveled along the polymer backbone. The mechanism for base dedoping of polyaniline is different than that for acid doping and may account for the slower response times and smaller resistance changes. In addition to the emeraldine salt and base forms, polyaniline can exist in several different oxidation states, including the fully reduced leucoemeraldine form, the halfoxidized emeraldine form, and the fully oxidized pernigraniline form. The oxidation states can either be controlled by synthetic conditions or oxidation–reduction reactions; hydrazine is known to convert the emeraldine form to the leucoemeraldine form. The sensing mechanism for chloroform molecules sensing is that chloroform molecules are relatively small and can diffuse efficiently into the polymeric matrix, which expands the structure and decreases the conductivity of the film. Small alcohol molecules have a different response mechanism to polyaniline from those of halogenated solvents. They interact with the nitrogen atoms of polyaniline, leading to an expansion of the compact polymer chains into a linear form, thus decreasing the resistance of the film.

Craighead and co-workers [111] created individual polyaniline/poly(ethylene oxide) nanowire sensors for detecting $NH_3$ at concentrations as low as 0.5 ppm with rapid response and recovery time. Tseng and co-workers [112] demonstrated real-time electronic sensing in the gas phase and in solution using an array of polyaniline nanoframework–electrode junctions. This sensing device could be used for chemical sensing of HCl, $NH_3$ and ethanol vapor, and also for pH sensing of aqueous NaCl solutions.

Also of interest is the work of Boussaad and Tao [113] who studied a tuning-fork sensor based on a polymer wire (nitrocellulose/toluene sulfonamide formaldehyde resin). The wire was glued onto the prongs of the tuning fork; the diameter of a small portion of the wire was reduced down to 100–500 nm with a focused ion beam system. Exposing the polymer wire to ethanol vapor changed the resonance frequency and thus the oscillation amplitude. The amplitude recovered after removing the vapor source and flushing the chamber with $N_2$. The change for 30 ppm was quicker and larger than that for 15 ppm. The authors suggested that the adsorption of organic vapors changed both the mass and the spring constant of the polymer wire.

### 5.5. Other nanowire sensor

Lieber et al. [114] reported optical studies of individual free-standing InP nanowires that demonstrated giant polarization anisotropy in photoluminescence (PL) measurements and the use of these InP nanowires as photoconductivity (PC)-based photodetectors. The PL properties of single InP nanowires recorded at room temperature with the polarization of the exciting laser parallel and perpendicular to the nanowire showed a giant polarization anisotropy. Wang and co-workers [115] fabricated $ZnSnO_3$ nanowire gas sensors which showed a very high sensitivity and sensitivity to 1 ppm ethanol at 300 °C. Both the response and the recovery time were about 1 s. Osterloh and co-workers [116] studied the conductivity of $LiMo_3Se_3$ nanowire films in the presence of organic vapors such as methanol, THF, acetonitrile, and DMSO. Zhou and co-workers [117] studied the photoconduction of single-crystal GaN nanowires. The nanowire transistors exhibited a substantial increase in conductance upon UV light exposure. Besides the selectivity to different light wavelengths, extremely short response and recovery time were also obtained, as well as the great reversibility of the nanowire between the high- and low-conductivity states.

## 6. Conclusion and remarks

This article provides a review on current research status of chemical sensors based on various new types of nanostructured materials such as nanotubes, nanorods, nanobelts, and nanowires. These nanostructure-based sensors represent a powerful detection platform for a broad range including biological sensors, electrochemical sensors, gas sensors, optical sensors, pH sensors, orientation sensors, etc. The sensing devices include individual nanostructured sensors, multi-nanostructured sensors, MOSFET-based sensors, and nanostructured film sensors, and so on. These nanosensor devices have a number of key features, including high sensitivity, exquisite selectivity, fast response and recovery, and potential for integration of addressable arrays on a massive scale, which sets them apart from other sensors technologies available today. In the near future, we argue that these advances could and should be developed at molecule level detection in simple nanosensor devices. However, there are still a lot of issues to be investigated:

(1) For sensing mechanism of nanosensors, many authors believe that it can be attributed to be high surface-to-volume ratios, porosity, small diameters, and the reactions between the oxygen species $O^{2-}$, $O^-$ and $O_2^-$ on the surface and samples. However, these aspects had been used for analyzing the sensing reactions long before, so we should explore the sensing mechanism in detail coupled with their special nanostructures. In addition, the chemical sensors based on nanostructured materials may have the required sensitivity,

but the selectivity of some kinds of sensors needs to be improved.

(2) Another important research topic is applications of nanosensors to security such as poison, drug (heroin), minim explosive, fire damp explosion in coal mine, nanoparticles in air, and so on, which would represent a clear application of nanotechnology and, more importantly, a substantial benefit to humankind.

(3) Finally, development of fabrication techniques of nanostructures coupled with other nano- and microstructures fabricated using "top down" techniques is needed. Especially for biosensor, for example, we believe that advances in capabilities of assembling larger and more complex nanosensor arrays and integrating them with first conventional and later nanoscale electronics for processing will lead to exquisitely powerful sensor systems that help to enable the potential on disease diagnosis, genetic screening, and drug discovery, as well as serve as powerful new tools for research in many areas of biology.

## Acknowledgement

This work was supported by Brain Korea 21 project, the School of Information Technology, Korea Advanced Institute of Science and Technology in 2006, and partially supported by Center for Ultramicrochemical Process Systems sponsored by KOSEF and the National Research and Development Program (NRDP, 2005-01274) for the biomedical function monitoring biosensor development sponsored by the Korea Ministry of Science and Technology (MOST).

## References

[1] T. Hyodo, J. Ohoka, Y. Shimizu, M. Egashira, Design of anodically oxidized $Nb_2O_5$ films as a diode-type $H_2$ sensing material, Sens. Actuators B, in press, corrected proof, available online 15 December 2005.

[2] T. Hyodo, K. Sasahara, Y. Shimizu, M. Egashira, Preparation of macroporous $SnO_2$ films using PMMA microspheres and their sensing properties to $NO_x$ and $H_2$, Sens. Actuators B 106 (2005) 580–590.

[3] L. Francioso, A. Forleo, S. Capone, M. Epifani, A.M. Taurino, P. Siciliano, Nanostructured $In_2O_3$—$SnO_2$ sol–gel thin film as material for $NO_2$ detection, Sens. Actuators B 114 (2006) 646–655.

[4] X.J. Huang, Y.K. Choi, K.S. Yun, E. Yoon, Oscillating behaviour of hazardous gas on tin oxide gas sensor: Fourier and wavelet transform analysis, Sens. Actuators B 115 (2006) 357–364.

[5] P. Ciosek, W. Wróblewski, The analysis of sensor array data with various pattern recognition techniques, Sens. Actuators B 114 (2006) 85–93.

[6] X.J. Huang, L.C. Wang, Y.F. Sun, F.L. Meng, J.H. Liu, Quantitative analysis of pesticide residue based on the dynamic response of a single $SnO_2$ gas sensor, Sens. Actuators B 99 (2004) 330–335.

[7] X.J. Huang, F.L. Meng, Z.X. Pi, W.H. Xu, J.H. Liu, Gas sensing behavior of a single tin dioxide sensor under dynamic temperature modulation, Sens. Actuators B 99 (2004) 444–450.

[8] X.J. Huang, J.H. Liu, D.L. Shao, Z.X. Pi, Z.L. Yu, Rectangular mode of operation for detecting pesticide residue by using a single $SnO_2$-based gas sensor, Sens. Actuators B 96 (2003) 630–635.

[9] X.J. Huang, J.H. Liu, Z.X. Pi, Z.L. Yu, Qualitative and quantitative analysis of organophosphorus pesticide residues using temperature modulated $SnO_2$ gas sensor, Talanta 64 (2004) 538–545.

[10] K.E. Sapsford, M.M. Ngundi, M.H. Moore, M.E. Lassman, L.C. Shriver-Lake, C.R. Taitt, F.S. Ligler, Rapid detection of food-borne contaminants using an array biosensor, Sens. Actuators B 113 (2006) 599–607.

[11] K.T.C. Chai, P.A. Hammond, D.R.S. Cumming, Modification of a CMOS microelectrode array for a bioimpedance imaging system, Sens. Actuators B 111–112 (2005) 305–309.

[12] T. Hyodo, T. Mori, A. Kawahara, H. Katsuki, Y. Shimizu, M. Egashira, Gas sensing properties of semiconductor heterolayer sensors fabricated by slide-off transfer printing, Sens. Actuators B 77 (2001) 41–47.

[13] P. Thiébaud, C. Beuret, N.F. de Rooij, M. Koudelka-Hep, Microfabrication of Pt-tip microelectrodes, Sens. Actuators B 70 (2000) 51–56.

[14] E. Llobet, P. Ivanov, X. Vilanova, J. Brezmes, J. Hubalek, K. Malysz, I. Gràcia, C. Cané, X. Correig, Screen-printed nanoparticle tin oxide films for high-yield sensor microsystems, Sens. Actuators B 96 (2003) 94–104.

[15] L.M. Cukrov, P.G. McCormick, K. Galatsis, W. Wlodarski, Gas sensing properties of nanosized tin oxide synthesised by mechanochemical processing, Sens. Actuators B 77 (2001) 491–495.

[16] V.V. Kissine, S.A. Voroshilov, V.V. Sysoev, Oxygen flow effect on gas sensitivity properties of tin oxide film prepared by r.f. sputtering, Sens. Actuators B 55 (1999) 55–59.

[17] R. Rella, A. Serra, P. Siciliano, L. Vasanelli, G. De, A. Licciulli, A. Quirini, Tin oxide-based gas sensors prepared by the sol–gel process, Sens. Actuators B 44 (1997) 462–467.

[18] X.J. Huang, Y.F. Sun, L.C. Wang, F.L. Meng, J.H. Liu, Carboxylation multi-walled carbon nanotubes modified with $LiClO_4$ for water vapour detection, Nanotechnology 15 (2004) 1284–1288.

[19] E. Chow, E.L.S. Wong, T. Böcking, Q.T. Nguyen, D.B. Hibbert, J.J. Gooding, Analytical performance and characterization of MPA-Gly-Gly-His modified sensors, Sens. Actuators B 111–112 (2005) 540–548.

[20] W.Y. Li, L.N. Xu, J. Chen, $Co_3O_4$ nanomaterials in lithium-ion batteries and gas sensors, Adv. Funct. Mater. 15 (2005) 851–857.

[21] J. Chen, L.N. Xu, W.Y. Li, X.L. Gou, $\alpha$-$Fe_2O_3$ nanotubes in gas sensor and lithium-ion battery applications, Adv. Mater. 17 (2005) 582–586.

[22] Y. Liu, M.L. Liu, Growth of aligned square-shaped $SnO_2$ tube arrays, Adv. Funct. Mater. 15 (2005) 57–62.

[23] J. Huang, N. Matsunaga, K. Shimanoe, N. Yamazoe, T. Kunitake, Nanotubular $SnO_2$ templated by cellulose fibers: synthesis and gas sensing, Chem. Mater. 17 (2005) 3513–3518.

[24] G.K. Mor, M.A. Carvalho, O.K. Varghese, M.V. Pishko, C.A. Grimes, A room-temperature $TiO_2$-nanotube hydrogen sensor able to self-clean photoactively from environmental contamination, J. Mater. Res. 19 (2004) 628–634.

[25] O.K. Varghese, D.W. Gong, M. Paulose, K.G. Ong, E.C. Dickey, C.A. Grimes, Extreme changes in the electrical resistance of titania nanotubes with hydrogen exposure, Adv. Mater. 15 (2003) 624–627.

[26] O.K. Varghese, D.W. Gong, M. Paulose, K.G. Ong, C.A. Grimes, Hydrogen sensing using titania nanotubes, Sens. Actuators B 93 (2003) 338–344.

[27] O.K. Varghese, C.A. Grimes, Metal oxide nanoarchitectures for environmental sensing, J. Nanosci. Nanotechnol. 3 (2003) 277–293.

[28] J.H. Yuan, K. Wang, X.H. Xia, Highly ordered platinum-nanotubule arrays for amperometric glucose sensing, Adv. Funct. Mater. 15 (2005) 803–809.

[29] C.H. Wang, X.F. Chu, M.M. Wu, Detection of $H_2S$ down to ppb levels at room temperature using sensors based on ZnO nanorods, Sens. Actuators B 113 (2006) 320–323.

[30] O. Wan, Q.H. Li, J.Y. Chen, H.T. Wang, X.L. He, J.P. Li, C.L. Lin, Fabrication and ethanol sensing characteristics of ZnO nanowire gas sensors, Appl. Phys. Lett. 84 (2004) 3654–3656.

[31] J.A. Dean, Lange's Handbook of Chemistry, Chinese ed., Science Press, 2003, pp. 43–54 (Chapter 4).

[32] B.S. Kang, Y.W. Heo, L.C. Tien, D.P. Norton, F. Ren, B.P. Gila, S.J. Pearton, Hydrogen and ozone gas sensing using multiple ZnO nanorods, Appl. Phys. A 80 (2005) 1029–1032.

[33] B.S. Kang, F. Ren, Y.W. Heo, L.C. Tien, D.P. Norton, S.J. Pearton, pH measurements with single ZnO nanorods integrated with a microchannel, Appl. Phys. Lett. 86 (2005) 112105–112107.

[34] H.T. Wang, B.S. Kang, F. Ren, L.C. Tien, P.W. Sadik, D.P. Norton, S.J. Pearton, J. Lin, Hydrogen-selective sensing at room temperature with ZnO nanorods, Appl. Phys. Lett. 86 (2005) 243503–243505.

[35] T. Gao, T.H. Wang, Synthesis and properties of multipod-shaped ZnO nanorods for gas-sensor applications, Appl. Phys. A 80 (2005) 1451–1454.
[36] Y. Dai, Y. Zhang, Q.K. Li, C.W. Nan, Synthesis and optical properties of tetrapod-like zinc oxide nanorods, Chem. Phys. Lett. 358 (2002) 83–86.
[37] J.Q. Xu, Y.P. Chen, D.Y. Chen, J.N. Shen, Hydrothermal synthesis and gas sensing characters of ZnO nanorods, Sens. Actuators B 113 (2006) 526–531.
[38] J.Q. Xu, Y.P. Chen, Y.D. Li, J.N. Shen, Gas sensing properties of ZnO nanorods prepared by hydrothermal method, J. Mater. Sci. 40 (2005) 2919–2921.
[39] F.F. Zhang, X.L. Wang, S.Y. Ai, Z.D. Sun, Q. Wan, Z.Q. Zhu, Y.Z. Xian, L.T. Jin, K. Yamamoto, Immobilization of uricase on ZnO nanorods for a reagentless uric acid biosensor, Anal. Chim. Acta 519 (2004) 155–160.
[40] E. Comini, L. Yubao, Y. Brando, G. Sberveglieri, Gas sensing properties of $MoO_3$ nanorods to CO and $CH_3OH$, Chem. Phys. Lett. 407 (2005) 368–371.
[41] Y.S. Kim, S.C. Ha, K. Kim, H. Yang, S.Y. Choi, Y.T. Kim, J.T. Park, C.H. Lee, J. Choi, J. Paek, K. Lee, Room-temperature semiconductor gas sensor based on nonstoichiometric tungsten oxide nanorod film, Appl. Phys. Lett. 86 (2005) 213105–213107.
[42] P.K. Sudeep, S.T. Shibu Joseph, K. George Thomas, Selective detection of cysteine and glutathione using gold nanorods, J. Am. Chem. Soc. 127 (2005) 6516–6517.
[43] C. Sönnichsen, A.P. Alivisatos, Gold nanorods as novel nonbleaching plasmon-based orientation sensors for polarized single-particle microscopy, Nano Lett. 5 (2005) 301–304.
[44] J. Jang, M. Chang, H. Yoon, Chemical sensors based on highly conductive poly(3,4-ethylene-dioxythiophene) nanorods, Adv. Mater. 17 (2005) 1616–1620.
[45] M.S. Arnold, P. Avouris, Z.W. Pan, Z.L. Wang, Field-effect transistors based on single semiconducting oxide nanobelts, J. Phys. Chem. B 107 (2003) 659–663.
[46] C. Yu, Q. Hao, S. Saha, L. Shi, X.Y. Kong, Z.L. Wang, Integration of metal oxide nanobelts with microsystems for nerve agent detection, Appl. Phys. Lett. 86 (2005) 063101.
[47] E. Comini, G. Faglia, G. Sberveglieri, Z.W. Pan, Z.L. Wang, Stable and highly sensitive gas sensors based on semiconducting oxide nanobelts, Appl. Phys. Lett. 81 (2002) 1869–1871.
[48] M. Law, H. Kind, B. Messer, F. Kim, P.D. Yang, Photochemical sensing of $NO_2$ with $SnO_2$ nanoribbon nanosensors at room temperature, Angew. Chem. Int. Ed. 41 (2002) 2405–2408.
[49] A. Maiti, J.A. Rodriguez, M. Law, P. Kung, J.R. McKinney, P.D. Yang, $SnO_2$ nanoribbons as $NO_2$ sensors: insights from first principles calculations, Nano Lett. 3 (2003) 1025–1028.
[50] A. Kolmakov, D.O. Klenov, Y. Lilach, S. Stemmer, M. Moskovits, Enhanced gas sensing by individual $SnO_2$ nanowires and nanobelts functionalized with Pd catalyst particles, Nano Lett. 5 (2005) 667–673.
[51] G. Faglia, C. Baratto, G. Sberveglieri, M. Zha, A. Zappettini, Adsorption effects of $NO_2$ at ppm level on visible photoluminescence response of $SnO_2$ nanobelts, Appl. Phys. Lett. 86 (2005) 011923–011925.
[52] T. Gao, T.H. Wang, Sonochemical synthesis of $SnO_2$ nanobelt/CdS nanoparticle core/shell heterostructures, Chem. Commun. (2004) 2558–2559.
[53] X.H. Kong, Y.D. Li, High sensitivity of CuO modified $SnO_2$ nanoribbons to $H_2S$ at room temperature, Sens. Actuators B 105 (2005) 449–453.
[54] E. Comini, G. Faglia, G. Sberveglieri, D. Calestani, L. Zanotti, M. Zha, Tin oxide nanobelts electrical and sensing properties, Sens. Actuators B 111–112 (2005) 2–6.
[55] J.F. Liu, X. Wang, Q. Peng, Y.D. Li, Vanadium pentoxide nanobelts: highly selective and stable ethanol sensor materials, Adv. Mater. 17 (2005) 764–767.
[56] F. Favier, E.C. Walter, M.P. Zach, T. Benter, R.M. Penner, Hydrogen sensors and switches from electrodeposited palladium mesowire arrays, Science 293 (2001) 2227–2231.
[57] B.J. Murray, E.C. Walter, R.M. Penner, Amine vapor sensing with silver mesowires, Nano Lett. 4 (2004) 665–670.
[58] E.C. Walter, F. Favier, R.M. Penner, Palladium mesowire arrays for fast hydrogen sensors and hydrogen-actuated switches, Anal. Chem. 74 (2002) 1546–1553.
[59] M. Yun, N.V. Myung, R.P. Vasquez, C. Lee, E. Menke, R.M. Penner, Electrochemically grown wires for individually addressable sensor arrays, Nano Lett. 4 (2004) 419–422.
[60] M.Z. Atashbar, S. Singamaneni, Room temperature gas sensor based on metallic nanowires, Sens. Actuators B 111–112 (2005) 13–21.
[61] A. Tao, F. Kim, C. Hess, J. Goldberger, R.R. He, Y.G. Sun, Y.N. Xia, P.D. Yang, Langmuīr–Blodgett silver nanowire monolayers for molecular sensing using surface-enhanced Raman spectroscopy, Nano Lett. 3 (2003) 1229–1233.
[62] C.Z. Li, H.X. He, A. Bogozi, J.S. Bunch, N.J. Tao, Molecular detection based on conductance quantization of nanowires, Appl. Phys. Lett. 76 (2000) 1333–1335.
[63] Y. Cui, Q.Q. Wei, H. Park, C.M. Lieber, Nanowire nanosensors for highly sensitive and selective detection of biological and chemical species, Science 293 (2001) 1289–1892.
[64] Y. Huang, X.F. Duan, Q.Q. Wei, C.M. Lieber, Directed assembly of one-dimensional nanostructures into functional networks, Science 291 (2001) 630–633.
[65] J. Hahm, C.M. Lieber, Direct ultrasensitive electrical detection of DNA and DNA sequence variations using nanowire nanosensors, Nano Lett. 4 (2004) 51–54.
[66] F. Patolsky, G.F. Zheng, O. Hayden, M. Lakadamyali, X.W. Zhuang, C.M. Lieber, Electrical detection of single viruses, PNAS 101 (2004) 14017–14022.
[67] W.U. Wang, C. Chen, K.H. Lin, Y. Fang, C.M. Lieber, Label-free detection of small-molecule–protein interactions by using nanowire nanosensors, PNAS 102 (2005) 3208–3212.
[68] X.T. Zhou, J.Q. Hu, C.P. Li, D.D.D. Ma, C.S. Lee, S.T. Lee, Silicon nanowires as chemical sensors, Chem. Phys. Lett. 369 (2003) 220–224.
[69] O.H. Elibol, D. Morisette, D. Akin, J.P. Denton, R. Bashir, Integrated nanoscale silicon sensors using top–down fabrication, Appl. Phys. Lett. 83 (2003) 4613–4615.
[70] J.F. Hsu, B.R. Huang, C.S. Huang, H.L. Chen, Silicon nanowires as pH sensor, Jpn. J. Appl. Phys. 44 (2005) 2626–2629.
[71] Z. Li, Y. Chen, X. Li, T.I. Kamins, K. Nauka, R.S. Williams, Sequence-specific label-free DNA sensors based on silicon nanowires, Nano Lett. 4 (2004) 245–247.
[72] Z. Li, B. Rajendran, T.I. Kamins, X. Li, Y. Chen, R.S. Williams, Silicon nanowires for sequence-specific DNA sensing: device fabrication and simulation, Appl. Phys. A 80 (2005) 1257–1263.
[73] J.T. Sheu, C.C. Chen, P.C. Huang, Y.K. Lee, M.L. Hsu, Selective deposition of gold nanoparticles on $SiO_2$/Si nanowires for molecule detection, Jpn. J. Appl. Phys. 44 (2005) 2864–2867.
[74] J. Lou, L.M. Tong, Z.Z. Ye, Modeling of silica nanowires for optical sensing, Opt. Express 13 (2005) 2135–2140.
[75] C. Li, D.H. Zhang, X.L. Liu, S. Han, T. Tang, J. Han, C.W. Zhou, $In_2O_3$ nanowires as chemical sensors, Appl. Phys. Lett. 82 (2003) 1613–1615.
[76] D.H. Zhang, C. Li, X.L. Liu, S. Han, T. Tang, C.W. Zhou, Doping dependent $NH_3$ sensing of indium oxide nanowires, Appl. Phys. Lett. 83 (2003) 1845–1847.
[77] C. Li, D.H. Zhang, B. Lei, S. Han, X.L. Liu, C.W. Zhou, Surface treatment and doping dependence of $In_2O_3$ nanowires as ammonia sensors, J. Phys. Chem. B 107 (2003) 12451–12455.
[78] D.H. Zhang, Z.Q. Liu, C. Li, T. Tang, X.L. Liu, S. Han, B. Lei, C.W. Zhou, Detection of $NO_2$ down to ppb levels using individual and multiple $In_2O_3$ nanowire devices, Nano Lett. 4 (2004) 1919–1924.
[79] J. Kong, N.R. Franklin, C.W. Zhou, M.G. Chapline, S. Peng, K. Cho, H.J. Dai, Nanotube molecular wires as chemical sensors, Science 287 (2000) 622–625.
[80] C. Li, B. Lei, D.H. Zhang, X.L. Liu, S. Han, T. Tang, M. Rouhanizadeh, T. Hsiai, C.W. Zhou, Chemical gating of $In_2O_3$ nanowires by organic and biomolecules, Appl. Phys. Lett. 83 (2003) 4014–4016.
[81] T. Tang, X.L. Liu, C. Li, B. Lei, D.H. Zhang, M. Rouhanizadeh, T. Hsiai, C.W. Zhou, Complementary response of $In_2O_3$ nanowires and carbon

nanotubes to low-density lipoprotein chemical gating, Appl. Phys. Lett. 86 (2005) 103903–103905.
[82] M. Curreli, C. Li, Y.H. Sun, B. Lei, M.A. Gundersen, M.E. Thompson, C.W. Zhou, Selective functionalization of $In_2O_3$ nanowire mat devices for biosensing applications, J. Am. Chem. Soc. 127 (2005) 6922–6923.
[83] D. Zhang, C. Li, S. Han, X. Liu, T. Tang, W. Jin, C.W. Zhou, Ultraviolet photodetection properties of indium oxide nanowires, Appl. Phys. A 77 (2003) 163–166.
[84] X.F. Chu, C.H. Wang, D.L. Jiang, C.M. Zheng, Ethanol sensor based on indium oxide nanowires prepared by carbothermal reduction reaction, Chem. Phys. Lett. 399 (2004) 461–464.
[85] A. Kolmakov, Y.X. Zhang, G.S. Cheng, M. Moskovits, Detection of CO and $O_2$ using tin oxide nanowire sensors, Adv. Mater. 15 (2003) 997–1000.
[86] Y. Zhang, A. Kolmakov, S. Chretien, H. Metiu, M. Moskovits, Control of catalytic reactions at the surface of a metal oxide nanowire by manipulating electron density inside it, Nano Lett. 4 (2004) 403–407.
[87] Y. Zhang, A. Kolmakov, Y. Lilach, M. Moskovits, Electronic control of chemistry and catalysis at the surface of an individual tin oxide nanowire, J. Phys. Chem. B 109 (2005) 1923–1929.
[88] Y.L. Wang, X.C. Jiang, Y.N. Xia, A solution-phase, precursor route to polycrystalline $SnO_2$ nanowires that can be used for gas sensing under ambient conditions, J. Am. Chem. Soc. 125 (2003) 16176–16177.
[89] C. Baratto, E. Comini, G. Faglia, G. Sberveglieri, M. Zha, A. Zappettini, Metal oxide nanocrystals for gas sensing, Sens. Actuators B 109 (2005) 2–6.
[90] Q. Wan, T.H. Wang, Single-crystalline Sb-doped $SnO_2$ nanowires: synthesis and gas sensor application, Chem. Commun. (2005) 3841–3843.
[91] N.S. Ramgir, I.S. Mulla, K.P. Vijayamohanan, A room temperature nitric oxide sensor actualized from Ru-doped $SnO_2$ nanowires, Sens. Actuators B 107 (2005) 708–715.
[92] S. Mathur, S. Barth, H. Shen, J.C. Pyun, U. Werner, Size-dependent photoconductance in $SnO_2$ nanowires, Small 1 (2005) 713–717.
[93] Q. Wan, Q.H. Li, Y.J. Chen, T.H. Wang, X.L. He, J.P. Li, C.L. Lin, Fabrication and ethanol sensing characteristics of ZnO nanowire gas sensors, Appl. Phys. Lett. 84 (2004) 3654–3656.
[94] Q.H. Li, Y.X. Liang, Q. Wan, T.H. Wang, Oxygen sensing characteristics of individual ZnO nanowire transistors, Appl. Phys. Lett. 85 (2004) 6389–6391.
[95] Z.Y. Fan, D.W. Wang, P.C. Chang, W.Y. Tseng, J.G. Lu, ZnO nanowire field-effect transistor and oxygen sensing property, Appl. Phys. Lett. 85 (2004) 5923–5925.
[96] Q. Wan, Q.H. Li, Y.J. Chen, T.H. Wang, X.L. He, X.G. Gao, J.P. Li, Positive temperature coefficient resistance and humidity sensing properties of Cd-doped ZnO nanowires, Appl. Phys. Lett. 84 (2004) 3085–3087.
[97] Y.S. Zhang, K. Yu, D.S. Jiang, Z.Q. Zhu, H.R. Geng, L.Q. Luo, Zinc oxide nanorod and nanowire for humidity sensor, Appl. Surf. Sci. 242 (2005) 212–217.
[98] Z.Y. Fan, J.G. Lu, Gate-refreshable nanowire chemical sensors, Appl. Phys. Lett. 86 (2005) 123510–123512.
[99] X.H. Wang, J. Zhang, Z.Q. Zhu, Ammonia sensing characteristics of ZnO nanowires studied by quartz crystal microbalance, Appl. Surf. Sci. 252 (2006) 2404–2411.
[100] L.C. Tien, H.T. Wang, B.S. Kang, F. Ren, P.W. Sadik, D.P. Norton, S.J. Pearton, J.S. Lin, Room-temperature hydrogen-selective sensing using single Pt-coated ZnO nanowires at microwatt power levels, Electrochem. Solid State Lett. 8 (2005) G230–G232.
[101] H. Kind, H.Q. Yan, B. Messer, M. Law, P.D. Yang, Nanowire ultraviolet photodetectors and optical switches, Adv. Mater. 14 (2002) 158–160.
[102] P.D. Yang, H.Q. Yan, S. Mao, R. Russo, J. Johnson, R. Saykally, N. Morris, J. Pham, R.R. He, H.J. Choi, Controlled growth of ZnO nanowires and their optical properties, Adv. Funct. Mater. 12 (2002) 323–331.
[103] M.F. Yu, M.Z. Atashbar, X.L. Chen, Mechanical and electrical characterization of β-$Ga_2O_3$ nanostructures for sensing applications, IEEE Sens. J. 5 (2005) 20–25.
[104] C.C. Chen, C.C. Chen, Morphology and electrical properties of pure and Ti-doped gas-sensitive $Ga_2O_3$ film prepared by rheotaxial growth and thermal oxidation, J. Mater. Res. 19 (2004) 1105–1117.
[105] H.Y. Yu, B.H. Kang, U.H. Pi, C.W. Park, S.Y. Choi, G.T. Kim, $V_2O_5$ nanowire-based nanoelectronic devices for helium detection, Appl. Phys. Lett. 86 (2005) 253102.
[106] N.F. Mott, Conduction in glasses containing transition metal ions, J. Non-Cryst. Solids 1 (1968) 1–17.
[107] I. Raible, M. Burghard, U. Schlecht, A. Yasuda, T. Vossmeyer, $V_2O_5$ nanofibres: novel gas sensors with extremely high sensitivity and selectivity to amines, Sens. Actuators B 106 (2005) 730–735.
[108] D.G. Laing, H. Panhuber, R.I. Baxter, $V_2O_5$ nanofibres: novel gas sensors with extremely high sensitivity and selectivity to amines, Sens. Actuators B 106 (2005) 730–735.
[109] J.X. Huang, S. Virji, B.H. Weiller, R.B. Kaner, Polyaniline nanofibers: facile synthesis and chemical sensors, J. Am. Chem. Soc. 125 (2003) 314–315.
[110] S. Virji, J.X. Huang, R.B. Kaner, B.H. Weiller, Polyaniline nanofiber gas sensors: examination of response mechanisms, Nano Lett. 4 (2004) 491–496.
[111] H.Q. Liu, J. Kameoka, D.A. Czaplewski, H.G. Craighead, Polymeric nanowire chemical sensor, Nano Lett. 4 (2004) 671–675.
[112] J. Wang, S. Chan, R.R. Carlson, Y. Luo, G. Ge, R.S. Ries, J.R. Heath, H.R. Tseng, Electrochemically fabricated polyaniline nanoframework electrode junctions that function as resistive sensors, Nano Lett. 4 (2004) 1693–1697.
[113] S. Boussaad, N.J. Tao, Polymer wire chemical sensor using a microfabricated tuning fork, Nano Lett. 3 (2003) 1173–1176.
[114] J.F. Wang, M.S. Gudiksen, X.F. Duan, Y. Cui, C.M. Lieber, Highly polarized photoluminescence and photodetection from single indium phosphide nanowires, Science 293 (2001) 1455–1457.
[115] X.Y. Xue, Y.J. Chen, Y.G. Wang, T.H. Wang, Synthesis and ethanol sensing properties of $ZnSnO_3$ nanowires, Appl. Phys. Lett. 86 (2005) 233101–233103.
[116] X.B. Qi, F.E. Osterloh, Chemical sensing with $LiMo_3Se_3$ nanowire films, J. Am. Chem. Soc. 127 (2005) 7666–7667.
[117] S. Han, W. Jin, D.H. Zhang, T. Tang, C. Li, X.L. Liu, Z.Q. Liu, B. Lei, C.W. Zhou, Photoconduction studies on GaN nanowire transistors under UV and polarized UV illumination, Chem. Phys. Lett. 389 (2004) 176–180.

## Biographies

**Xing-Jiu Huang** received his MS degree in Department of Chemistry from Wuhan University, China in 2001, and PhD in Department of Chemistry at University of Science and Technology of China in 2004. He is now working in Department of Electrical Engineering and Computer Science at Korea Advanced Institute of Science and Technology (KAIST), Korea, as a post-doctoral research fellow. His current research interests are nanoscale biosensors, chemical sensors, design of microfluidic chip and micro-TAS.

**Yang-Kyu Choi** received the BS and MS degree in Department of Physics from Seoul National University, South Korea, in 1989 and 1991, respectively. From 1997 to 1999, he studied in Electrical Engineering Department at University of California, Berkeley, and obtained his MS degree in 1999. He received his PhD degree in Department of Electrical Engineering and Computer Sciences at University of California, Berkeley, in 2001. From 2001 to 2003, he worked in University of California, Berkeley, as a post-doctoral researcher. In 2004, he joined the Department of Electrical Engineering at Korea Advanced Institute of Science and Technology (KAIST). His current research interests are nanoscale bioelectronics, biosensors, chemical sensors and DNA biochip.